



Cite this: *RSC Adv.*, 2018, 8, 5145

Received 20th November 2017  
Accepted 18th January 2018

DOI: 10.1039/c7ra12606a

rsc.li/rsc-advances

# OH<sup>-</sup> absorption and holographic storage properties of Sc(0, 1, 2, 3):Ru:Fe:LiNbO<sub>3</sub> crystals

Li Dai,<sup>a</sup> Luping Wang,<sup>b</sup> Chunrui Liu,<sup>a</sup> Xianbo Han,<sup>a</sup> Zhehua Yan<sup>a</sup> and Yuheng Xu<sup>b,c</sup>

A series of Sc:Ru:Fe:LiNbO<sub>3</sub> crystals with various levels of Sc<sub>2</sub>O<sub>3</sub> (0, 1, 2, and 3 mol%) doping were grown from congruent melts in air by using the Czochralski technique. The defect structures and photorefractive properties of the Sc:Ru:Fe:LiNbO<sub>3</sub> crystals were investigated by acquiring infrared spectra of the crystals and performing two-wavelength nonvolatile experiments, respectively. Our results showed the holographic storage properties of Ru:Fe:LiNbO<sub>3</sub> crystals to be enhanced by doping them with a high concentration of Sc<sub>2</sub>O<sub>3</sub>, and indicated Sc:Ru:Fe:LiNbO<sub>3</sub> crystals to constitute a promising medium for holographic storage.

## 1. Introduction

With excellent nonlinear optical, electro-optical, acoustic-optical, ferroelectric and photorefractive properties, LiNbO<sub>3</sub>- (LN) crystals have become very promising materials.<sup>1,2</sup> In the past few decades, due to its high storage capacity, fast parallel processing and content addressability, the LiNbO<sub>3</sub> crystal has garnered great interest,<sup>3</sup> and has been successfully applied in integrated electro-optical devices and holographic memory devices.<sup>4</sup> However, the volatility of stored information is a major obstacle in the practical application of LiNbO<sub>3</sub> crystals. In order to solve this problem, photorefractive ions such as those of Fe,<sup>5</sup> Ce,<sup>6</sup> Cu,<sup>7</sup> Ru,<sup>8</sup> Mn, Ti,<sup>9</sup> Er<sup>10–14</sup> are introduced into the crystal to enhance the photorefractive effect, and it was found that a nonvolatile readout can be realized in some doubly doped LiNbO<sub>3</sub>.<sup>15,16</sup>

Based on this development, a two-centered recording model was proposed in the doubly doped Fe:Mn:LiNbO<sub>3</sub> crystal by Buse *et al.* in 1998,<sup>17</sup> and holographic recording and nondestructive readout were implemented in Fe:Mn:LiNbO<sub>3</sub>. The key point of the technique is that the doped ions can provide both relatively shallow and deep centers in the crystals. Many new doubly doped crystals, such as Cu:Ce:LiNbO<sub>3</sub>, Mn:Ce:LiNbO<sub>3</sub> and Fe:Cu:LiNbO<sub>3</sub> crystals, have since been reported to have such properties.<sup>18,19</sup> The Ru:Fe:LiNbO<sub>3</sub> crystal was recently found to be another excellent medium for holographic storage. Fe and Ru are both transition metal ions and are located at similar positions of the periodic table; and in the Ru:Fe:LiNbO<sub>3</sub> crystal, Ru is used as a deep center and Fe as a shallow center.<sup>20</sup>

Generally speaking, the higher the concentration of the doping ion, the stronger the photorefractive effect; therefore, a lower response time, higher sensitivity, higher diffraction efficiency and other excellent parameters can be achieved by using a higher doping concentration. But it is not easy to grow large and high-quality Ru:Fe:LiNbO<sub>3</sub> crystals, because of the low solubility of Fe and Ru in the LiNbO<sub>3</sub> crystal. Comparatively speaking, doping ions resistant to optical damage is a more feasible method: it not only can eliminate the intrinsic defects caused by the Li composition deficiency but also can improve optical resistance ability of the crystal.

The choice of doping ions is critical for the characteristics and applications of LN crystals. In this work, the Sc<sup>3+</sup> (ref. 21–24) ion was chosen as the doping ion. The ionic radius of Sc<sup>3+</sup> is similar to that of Li<sup>+</sup> but larger than that of Nb<sup>5+</sup>, and the Sc<sup>3+</sup>-doped LN has been used in integrated optics such as titanium-diffused optical LN waveguides doped with Sc<sup>3+</sup>. The LN crystal is susceptible to photorefractive damage under laser irradiation. To suppress photorefractive damage, the LN crystal must be doped with more than 4.6 mol% Mg,<sup>25</sup> more than 6.2 mol% Zn,<sup>26</sup> more than 3 mol% In,<sup>27</sup> or more than 2 mol% Sc.<sup>28</sup> We chose Sc<sup>3+</sup> ion as the doping ion since it was effective at a concentration lower than were any of the other ions.

Based on the above considerations, a series of Sc:Ru:Fe:LiNbO<sub>3</sub> crystals with various concentrations of Sc<sub>2</sub>O<sub>3</sub> were grown by using the Czochralski method. The defect structures of Sc:Ru:Fe:LiNbO<sub>3</sub> crystals were investigated by acquiring their infrared spectra, and the holographic storage properties of Sc:Ru:Fe:LiNbO<sub>3</sub> were investigated by taking two-wavelength nonvolatile measurements.

## 2. Crystal growth

In our experiment, the Sc(0, 1, 2, and 3 mol%):Ru:Fe:LiNbO<sub>3</sub> crystals with 0.3 mol% Fe<sub>2</sub>O<sub>3</sub> and 0.2 mol% RuO<sub>2</sub> were grown

<sup>a</sup>College of Science, Harbin University of Science and Technology, Harbin 150080, China. E-mail: daili198108@126.com; Tel: +86 451 86390731

<sup>b</sup>School of Materials Science and Engineering, Harbin University of Science and Technology, Harbin 150040, China

<sup>c</sup>Department of the Applied Chemistry, Harbin Institute of Technology, Harbin 150001, China



from congruent melts in air by using the Czochralski technique. The raw materials used in crystal growth were  $\text{Nb}_2\text{O}_5$ ,  $\text{LiCO}_3$ ,  $\text{Sc}_2\text{O}_3$ ,  $\text{RuO}_2$  and  $\text{Fe}_2\text{O}_3$ . The purity of raw material is critical for optical quality, so the purity levels of all raw materials were at least 99.99%. All raw materials including  $\text{Nb}_2\text{O}_5$ ,  $\text{LiCO}_3$ ,  $\text{Sc}_2\text{O}_3$ ,  $\text{RuO}_2$  and  $\text{Fe}_2\text{O}_3$  were mixed for 24 hours in order to obtain uniform materials. Then the materials were placed into a platinum crucible heated up to  $750\text{ }^\circ\text{C}$  for 2 hours to remove  $\text{CO}_2$  and then heated up further to  $1150\text{ }^\circ\text{C}$  for 2 hours to form a polycrystalline material as a result of a solid-state reaction. The growth condition was selected as follows: the temperature gradient was  $2.5\text{ }^\circ\text{C mm}^{-1}$ , the polling rate and rotation rate were controlled to be in the range  $0.8$  to  $1.5\text{ mm h}^{-1}$  and  $17$ – $26\text{ rpm}$ , respectively. After growth, the crystals were cooled to room temperature at a rate of  $65\text{ }^\circ\text{C h}^{-1}$ . In order to prevent spontaneous polarization of the crystals, all of the crystals needed to be polarized artificially in a medium frequency furnace for 8 h, in which the temperature was  $1100\text{ }^\circ\text{C}$ , the temperature gradient was almost equal to zero, and the current density was  $5\text{ mA cm}^{-2}$ . Several  $8\text{ mm} \times 10\text{ mm} \times 2\text{ mm}$  ( $x \times y \times z$ ) wafers were obtained by cutting from the middle of the  $\text{Sc:Ru:Fe:LiNbO}_3$  crystals along the  $y$ -axis. The samples with different  $\text{Sc}^{3+}$  ion concentrations were labeled as  $\text{ScRuFe-0}$ , 1, 2 and 3. A photograph of one of the  $\text{ScRuFe-3}$  crystals is shown in Fig. 1.

### 3. Measurements

#### 3.1 Infrared absorption spectra of $\text{Sc:Ru:Fe:LiNbO}_3$ crystals

The water in the raw materials and growth atmosphere were expected to cause  $\text{H}^+$  ions to enter the crystal lattice and form O–H–O during the crystal growth. The frequency and energy of infrared light can only make molecules vibrate and their rotation levels change. Since the vibration of O–H is very sensitive to its environment, including surrounding ions, we expected the defects and structure of our crystals to be amenable to analysis using infrared spectroscopy.<sup>29</sup>

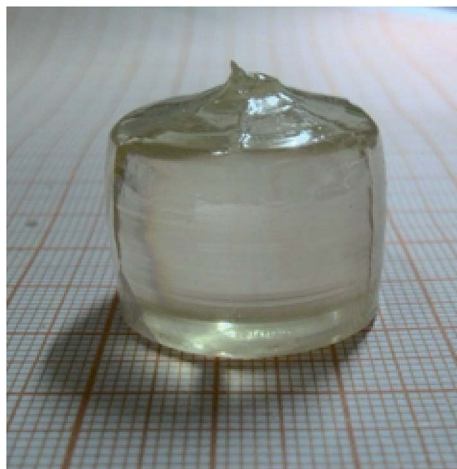


Fig. 1 A sample  $\text{ScRuFe-3}$  crystal.

The infrared absorption spectra of the crystals were each acquired in the wavenumber range  $3400\text{ cm}^{-1}$  to  $3540\text{ cm}^{-1}$  at room temperature. As shown in Fig. 2, the  $\text{OH}^-$  absorption bands of samples  $\text{ScRuFe-0}$ , 1 and 2 were all located at about  $3482\text{ cm}^{-1}$ , while the  $\text{OH}^-$  band of sample  $\text{ScRuFe-3}$  was located at  $3507\text{ cm}^{-1}$ . The shape of an  $\text{OH}^-$  absorption band is related to the crystal composition and ions surrounding the  $\text{OH}^-$ . The  $\text{OH}^-$  absorption band of  $\text{LiNbO}_3$  is also located at  $3482\text{ cm}^{-1}$ .<sup>30</sup>

The mechanism underlying the shift of the absorption peak can be described as follows. The  $[\text{Li}]/[\text{Nb}]$  ratio in congruent  $\text{LiNbO}_3$  crystals has been previously indicated to be about 0.946, and to have caused the generation of intrinsic defects. During the growth of such crystals, a lattice position missing the  $\text{Li}^+$  ion would form a Li vacancy  $V_{\text{Li}}^-$ , which would be filled by a  $\text{Nb}^{3+}$  ion to form an anti site  $\text{Nb}_{\text{Li}}^{4+}$ . The concentration threshold of anti-photorefractive can be defined as that when the doped ions enter the normal Nb position. In our experiment, the concentrations of  $\text{Fe}^{3+}$  and  $\text{Ru}^{4+}$  ions were fixed, so we just took the  $\text{Sc}^{3+}$  ion into account; as indicated above, the concentration threshold of  $\text{Sc}^{3+}$  ions has been reported to be 2 mol%. The concentrations of  $\text{Sc}_2\text{O}_3$  added into the growth melts of samples  $\text{ScRuFe-0}$ , 1, 2 and 3 were measured using ICP-AES spectrometry to be 0 mol%, 0.78 mol%, 1.44 mol% and 2.07 mol% respectively. For the  $\text{Sc:Ru:Fe:LiNbO}_3$  crystals with a dopant concentration below its threshold value, the doping Sc, Ru and Fe ions, according to the proposed mechanism, replaced  $\text{Nb}_{\text{Li}}^{4+}$  and  $V_{\text{Li}}^-$  to form the defects  $\text{Sc}_{\text{Li}}^{2+}$ ,  $\text{Ru}_{\text{Li}}^{4+}$  and  $\text{Fe}_{\text{Li}}^{2+}$ , respectively. Due to the repulsion between these ions and  $\text{H}^+$ , the  $\text{H}^+$  ions were still attracted by  $V_{\text{Li}}^-$ , which caused the  $\text{OH}^-$  absorption bands of samples  $\text{ScRuFe-0}$ , 1, 2 to be quite similar. According to the proposed mechanism, for the concentration of  $\text{Sc}^{3+}$  ions exceeding the threshold,  $\text{Sc}^{3+}$  occupied Nb sites and formed the defect  $\text{Sc}_{\text{Nb}}^{2-}$ .  $\text{Sc}_{\text{Nb}}^{2-}$  attracts  $\text{H}^+$  ions more strongly than does  $V_{\text{Li}}^-$ , so the  $\text{H}^+$  ions gathered near  $\text{Sc}_{\text{Nb}}^{2-}$  according to our proposal. The shift of the absorption band of sample  $\text{ScRuFe-3}$  to  $3507\text{ cm}^{-1}$  was attributed to the above mechanism. Note also

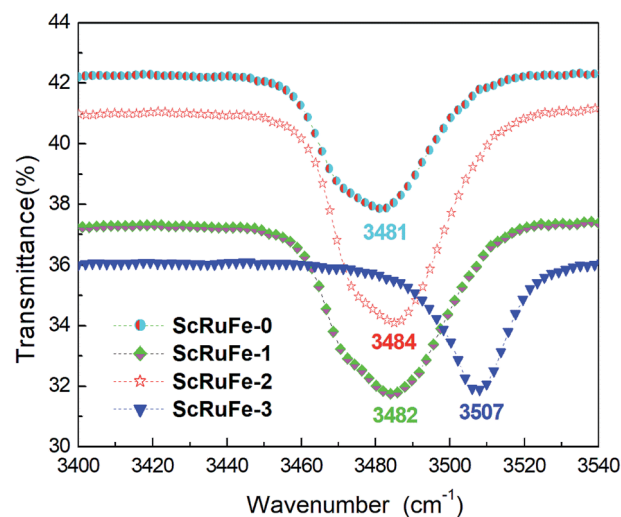


Fig. 2 Infrared transmittance spectra of  $\text{Sc:Ru:Fe:LiNbO}_3$  crystals.



that the OH<sup>-</sup> absorption band of sample ScRuFe-3 was sharper than those of the others, and this observation was attributed to the formation of more Sc<sub>Nb</sub><sup>2-</sup> defects resulting from the higher concentration of Sc<sup>3+</sup> in this sample.

### 3.2 Two-wavelength nonvolatile measurements

Two-wavelength nonvolatile measurements were taken to study the holographic storage properties of the Sc:Ru:Fe:LiNbO<sub>3</sub> crystals. The experimental setup is shown in Fig. 3. A Kr<sup>+</sup> laser with λ = 476 nm and an He-Ne laser with λ = 633 nm were used as the recording and readout beams, respectively. By using a continuously adjustable beam splitter, the recording beam was split into two beams, I<sub>S</sub> and I<sub>R</sub>, of equal 120 mW cm<sup>-2</sup> intensity. The two beams were then polarized in the incidence plane, and then directed to the crystal at the corresponding Bragg angle of 16°. The two beams intersected symmetrically inside the crystal and made the grating vector along the *c*-axis. During the recording process, the two beams were first directed onto the crystal at the same time, and then the beam I<sub>S</sub> was blocked from time to time by a shutter, and the diffraction efficiency of another beam I<sub>R</sub> was detected for a short duration of 10 s in order to eliminate the impact of erasure. After the grating store was saturated, I<sub>S</sub> and I<sub>R</sub> were both blocked only by the He-Ne beam directed onto the sample, and the intensities of transmitted I<sub>t</sub> and diffracted I<sub>d</sub> were determined. This process was the nonvolatile readout. By carrying out these experiments, the holographic storage properties of the samples were determined.

Next we discuss the holographic storage properties of the Sc:Ru:Fe:LiNbO<sub>3</sub> crystals.

The diffraction efficiency η was defined as, the diffraction efficiency η was defined as

$$\eta = I_d/I_t \times 100\% \quad (1)$$

where I<sub>t</sub> is the transmitted light intensity and I<sub>d</sub> the diffracted light intensity of the readout beam.

$$\sqrt{\eta} = \sqrt{\eta_{\text{sat}}}(1 - \exp(-t/\tau_w)) \quad (2)$$

The recording and erasure time constants were described by using eqn (2) and (3).

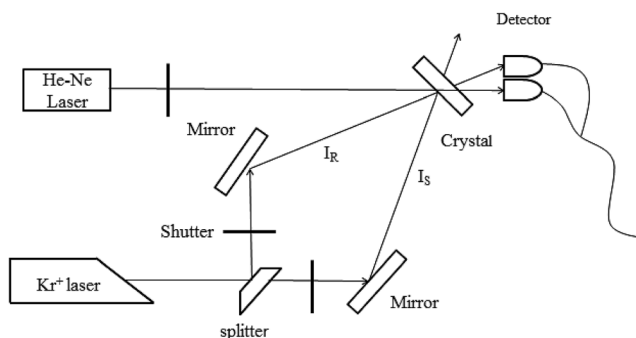


Fig. 3 Two-wavelength nonvolatile experiment setup.

$$\sqrt{\eta} = \sqrt{\eta_{\text{sat}}}(1 - \exp(-t/\tau_e)) \quad (3)$$

In these equations, τ<sub>w</sub> and τ<sub>e</sub> are the recording and erasure time constants respectively. Also, η<sub>sat</sub> is the saturation diffraction efficiency during recording, and it was fixed by the function

$$\eta_{\text{max}} = \sin^2\left(\frac{\pi d \Delta \eta_{\text{sat}}}{\lambda \cos \theta_{\text{cry}}}\right) \quad (4)$$

where η<sub>max</sub> is the maximum value of diffraction efficiency, *d* is the thickness of the samples, λ is the wavelength of the recording beam, and θ<sub>cry</sub> is the refraction angle of incidence light within the crystal.

Sensitivity (*S*) and its dynamic range (*M*/#) were calculated using eqn (5) and (6).<sup>31,32</sup>

$$S = \left[\frac{d\sqrt{\eta}}{dt}\right]_{t=0} / IL \approx \sqrt{\eta_s} / (\tau_w \times IL) \quad (5)$$

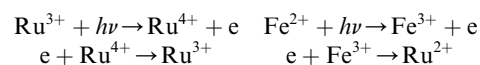
$$M/\# = \tau_e \left[\frac{d\sqrt{\eta}}{dt}\right]_{t=0} \approx \frac{\tau_e}{\tau_w} \sqrt{\eta_s} \quad (6)$$

In these equations, *I* is the total optical intensity, and *L* is the crystal plate thickness.

The dual-wavelength nonvolatile holographic recording-readout curves are shown in Fig. 4.

The holographic storage parameters of the Sc:Ru:Fe:LiNbO<sub>3</sub> crystals measured by performing the dual-wavelength experiment are listed in Table 1. The results showed that the holographic storage parameters improved as the Sc<sub>2</sub>O<sub>3</sub> doping concentration was increased. Compared to the values of ScRuFe-0, τ<sub>w</sub> of ScRuFe-3 decreased by a factor of 3.0, η<sub>s</sub> increased by a factor of 1.6, *S* increased by a factor of 4, and *M*/# increased by a factor of 7.9. The η<sub>s</sub>, *S*, and *M*/# values of sample ScRuFe-3 were in fact higher than the corresponding values of the other tested samples.

The holographic storage properties of the Sc:Ru:Fe:LiNbO<sub>3</sub> crystal are known to depend on the photorefractive sensitive center. In this crystal, there are two photorefractive ions, Ru<sup>4+</sup> and Fe<sup>3+</sup>, which can form deep and shallow trap centers, respectively. The Sc<sup>3+</sup> ion has a stable single valence state, so it cannot form a photorefractive center. First we discuss the carrier transport model in Sc:Ru:Fe:LiNbO<sub>3</sub> crystals. Here, Ru and Fe both have two different valences, which can form a donor level and acceptor level. Ru<sup>3+</sup> and Fe<sup>2+</sup> ions can bind many donor level electrons, while Ru<sup>4+</sup> and Fe<sup>3+</sup> can bind almost no acceptor level electrons. When the incidence light was directed onto the crystal, the electrons in the donor level (Ru<sup>3+</sup> and Fe<sup>2+</sup>) were excited to the conduction band, and after drift and diffusion, they were absorbed by acceptor levels (Ru<sup>4+</sup> and Fe<sup>3+</sup>). The process can be described as follows:<sup>33</sup>



The Sc<sup>3+</sup> ion enter into the lattice of Ru:Fe:LiNbO<sub>3</sub> crystal has no direct influence on the formation of the grating. The photorefractive ions Fe<sup>2+</sup>/Fe<sup>3+</sup> and Ru<sup>3+</sup>/Ru<sup>4+</sup> play a dominate role in



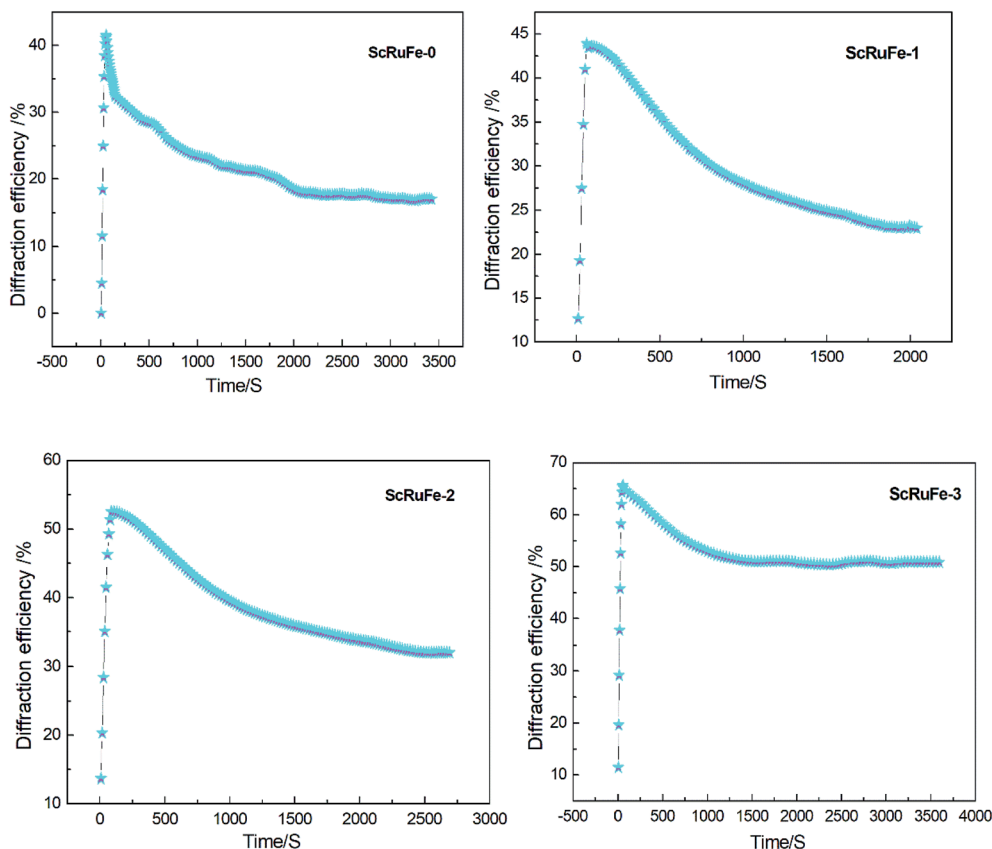


Fig. 4 Time dependence of diffraction efficiency during dual-wavelength nonvolatile holographic recording of the samples.

Table 1 Experimentally determined holographic storage properties of the Sc:Ru:Fe:LiNbO<sub>3</sub> crystals

Sample	$\tau_w$ (s)	$\tau_e$ (s)	$\eta_s$ (%)	$S$ (cm J <sup>-1</sup> )	$M/\#$	$\Delta n_s (\times 10^{-5})$	$\sigma_{ph} (\times 10^{-12} \text{ cm } \Omega^{-1} \text{ W}^{-1})$
ScRuFe-0	389.2	937.2	41.2	0.04	1.55	4.17	0.64
ScRuFe-1	275.1	1105.7	44.5	0.06	2.68	4.33	0.90
ScRuFe-2	210.5	1461.5	53.4	0.09	5.07	4.75	1.18
ScRuFe-3	128.9	1937.8	65.6	0.16	12.18	5.26	1.92

photo-excited carrier transport processes. Doped Sc<sup>3+</sup> ions influenced the ion arrangement and defects in the Sc:Ru:Fe:LiNbO<sub>3</sub> crystals, and a detailed mechanism for this influence was derived. According to this proposed mechanism, Sc<sup>3+</sup> ions at doping concentrations below its threshold concentration replaced the Nb<sub>Li</sub><sup>4+</sup> defects, while Sc<sup>3+</sup> ions at concentrations exceeding its threshold concentration replaced the normal Li position. Due to the polarization ability of the Sc<sup>3+</sup> ion being stronger than that of the Li<sup>+</sup> ion, the ability of Sc<sup>3+</sup> ions to capture electrons was also better than that for Li<sup>+</sup> ions. In the process, the trap density of the electron acceptor increased and the saturation diffraction efficiency  $\eta_{\text{sat}}$  was also improved. The equation mentioned above indicated the dynamic range  $M/\#$  to be approximately proportional to the saturation diffraction efficiency  $\eta_{\text{sat}}$ , so the dynamic range  $M/\#$  increased with increasing concentration of the doped Sc<sup>3+</sup> ions. For the LiNbO<sub>3</sub> crystal, the photoconductivity  $\sigma_{\text{ph}}$  has been shown to be related to the

electron traps and to be inversely proportional to the Nb<sub>Li</sub><sup>4+</sup> concentration. Increasing the concentration of the doped Sc<sup>3+</sup> ions led to a decrease in the concentration of Nb<sub>Li</sub><sup>4+</sup>, which in turn led to the increase in the photoconductivity  $\sigma_{\text{ph}}$  and decrease in the response time. Sensitivity  $S$  is the comprehensive measure of saturation diffraction efficiency  $\eta_{\text{sat}}$  and photoconductivity  $\sigma_{\text{ph}}$ . As the results showed, increasing the concentration of Sc<sup>3+</sup> doped into the Ru:Fe:LiNbO<sub>3</sub> crystals coincided with a decrease in writing time  $\tau_w$  and increases in the dynamic range  $M/\#$ , saturation diffraction efficiency  $\eta_{\text{sat}}$ , photoconductivity  $\sigma_{\text{ph}}$  and sensitivity  $S$ .

## 4. Conclusions

Sc:Ru:Fe:LiNbO<sub>3</sub> crystals with various concentrations of Sc<sup>3+</sup> were grown by using the Czochralski method. The OH<sup>-</sup> absorption experiment results showed the absorption bands of



samples ScRuFe-0, 1, 2 to all be located at a similar wave-number, of about  $3484\text{ cm}^{-1}$ , when the doping  $\text{Sc}^{3+}$  ion concentration was below its threshold concentration. Once the  $\text{Sc}^{3+}$  concentration exceeded its threshold value, *i.e.*, for ScRuFe-3, the absorption band shifted significantly, to  $3507\text{ cm}^{-1}$ . The two-wavelength nonvolatile experiment results demonstrated that the holographic storage properties improved with increasing  $\text{Sc}^{3+}$  concentration. Compared to the other samples, ScRuFe-3, *i.e.*, that with the highest  $\text{Sc}^{3+}$  doping concentration, showed the shortest response time, and the highest dynamic range  $M/\#$ , saturation diffraction efficiency  $\eta_{\text{sat}}$ , and sensitivity levels, which are key parameters of volume holographic data storage. These results indicated the Sc:Ru:Fe:LiNbO<sub>3</sub> crystals to be promising materials for nonvolatile holographic storage.

## Conflicts of interest

There are no conflicts to declare.

## Acknowledgements

This work is supported by the Youth Science Fund of Heilongjiang Province of China (No. QC2015061).

## References

- C. Xu, C. L. Zhang, L. Dai, *et al.*, OH<sup>-</sup> absorption and nonvolatile holographic storage properties in Mg:Ru:Fe:LiNbO<sub>3</sub> crystal as a function of Mg concentration, *Chin. Phys. B*, 2013, **22**(5), 306–309.
- C. Xu, X. Leng, Y. Mo, *et al.*, Investigations on growth and two-wavelength holographic storage properties varied with RuO<sub>2</sub>, codoping in Fe: LiNbO<sub>3</sub>, crystals, *J. Cryst. Growth*, 2011, **318**(1), 665–668.
- L. Dhar, K. Curtis and T. Fäcke, Holographic data storage: coming of age, *Nat. Photonics*, 2008, **2**, 9–11.
- D. Huang, J. Wang, J. Sun, *et al.*, Optical phase erasure and its application to format conversion through cascaded second-order processes in periodically poled lithium niobate, *Opt. Lett.*, 2008, **33**(16), 1804–1806.
- S. Kar, S. Verma and K. S. Bartwal, Growth Optimization and Optical Characteristics of Fe Doped LiNbO<sub>3</sub> Crystals, *Cryst. Growth Des.*, 2008, **8**(12), 4424–4427.
- X. G. Xu, G. B. Xu, D. W. Hu, *et al.*, Photorefractive Holographic Storage Properties in Ce:Fe-Doped LiNbO<sub>3</sub> Crystals, *Acta Opt. Sin.*, 2004, **24**(7), 947–952.
- I. Pracka, A. L. Bajor, S. M. Kaczmarek, *et al.*, Growth and Characterization of LiNbO<sub>3</sub> Single Crystals Doped with Cu and Fe Ions, *Cryst. Res. Technol.*, 2010, **34**(5–6), 627–634.
- C. H. Chiang and J. C. Chen, Growth and properties of Ru-doped lithium niobate crystal, *J. Cryst. Growth*, 2006, **294**(2), 323–329.
- L. Hesselink, S. S. Orlov, A. Liu, A. Akella, D. Lande and R. R. Neurgaonkar, Photorefractive materials for nonvolatile volume holographic data storage, *Science*, 1998, **282**(5391), 1089.
- Y. Tomita, M. Hoshi and S. Sunarno, Nonvolatile Two-Color Holographic Recording in Er-Doped LiNbO<sub>3</sub>, *Jpn. J. Appl. Phys.*, 2014, **40**(10), L1035–L1037.
- D. L. Zhang, J. Zhang, Z. K. Wu and E. Y. B. Pun, Light-induced absorption in reduced congruent and near-stoichiometric Er:LiNbO<sub>3</sub>, crystals, *Appl. Phys. A*, 2006, **83**(3), 397–409.
- C. H. Huang and L. McCaughan, 980-nm-pumped Er-doped LiNbO<sub>3</sub>, waveguide amplifiers: a comparison with 1484-nm pumping, *IEEE J. Sel. Top. Quantum Electron.*, 1996, **2**(2), 367–372.
- D. L. Zhang, J. Zhang, Y. F. Wang, D. S. Zhu, Z. K. Wu and E. Y. B. Pun, Light-induced absorption instability in weakly reduced congruent Er:LiNbO<sub>3</sub> crystal, *Appl. Phys. A*, 2005, **80**(8), 1819–1828.
- D. L. Zhang, Y. R. Zhuang, J. Zhang, Z. K. Wu and E. Y. B. Pun, Light-induced diffraction in thermally reduced congruent and near-stoichiometric Er:LiNbO<sub>3</sub> crystals, *J. Mod. Opt.*, 2005, **52**(15), 2105–2126.
- Q. Dong, L. Liu, D. Liu, *et al.*, Effect of dopant composition ratio on nonvolatile holographic recording in LiNbO<sub>3</sub>:Cu:Ce crystals, *Appl. Opt.*, 2004, **43**(26), 5016.
- C. Zhou, D. Liu, G. Li, *et al.*, Nonvolatile holograms in LiNbO<sub>3</sub>:Fe:Cu by use of the bleaching effect, *Appl. Opt.*, 2002, **41**(32), 6809.
- K. Buse, A. Adibi and D. Psaltis, Non-volatile holographic storage in doubly doped lithium niobate crystals, *Nature*, 1998, **393**(6686), 665–668.
- Y. Liu, L. Liu, D. Liu, *et al.*, Intensity dependence of two-center nonvolatile holographic recording in LiNbO<sub>3</sub>:Cu:Ce crystals, *Opt. Commun.*, 2001, **190**(1–6), 339–343.
- Y. Tomita, S. Sunarno and G. Zhang, Ultraviolet-light-gating two-color photorefractive effect in Mg-doped nearstoichiometric LiNbO<sub>3</sub>, *J. Opt. Soc. Am. A*, 2004, **21**, 753–760.
- C. Xu, C. Yang, C. Zhu, *et al.*, Improved nonvolatile holographic storage properties in Zr: Ru:Fe:LiNbO<sub>3</sub> crystal by blue light recording, *Mater. Lett.*, 2012, **67**(1), 320–322.
- D. L. Zhang, C. X. Qiu, W. H. Wong, *et al.*, Optical-Damage-Resistant Ti-Diffused LiNbO<sub>3</sub>, Strip Waveguide Doped with Scandium, *IEEE Photonics Technol. Lett.*, 2014, **26**(17), 1770–1773.
- D. L. Zhang, C. X. Qiu, W. H. Wong, *et al.*, Relation of Refractive Index Change to Ti-Concentration in Ti-Diffused LiNbO<sub>3</sub>, Waveguide Doped with Sc<sup>3+</sup>, *J. Lightwave Technol.*, 2014, **32**(15), 2666–2670.
- X. F. Yang, Z. B. Zhang, W. Y. Du, *et al.*, Near-stoichiometric Ti:Sc:LiNbO<sub>3</sub> strip waveguide for integrated optics, *Opt. Mater. Express*, 2016, **6**(8), 2637.
- D. L. Zhang, Q. Zhang, C. X. Qiu, *et al.*, Control of scandium diffusion in LiNbO<sub>3</sub>, single crystal by co-diffusion of titanium, *J. Mater. Sci.*, 2015, **50**(12), 4149–4159.
- D. A. Bryan, R. Gerson and H. E. Tomaschke, *Increased optical damage resistance in lithium niobate*, *Appl. Phys. Lett.*, 1984, **44**(9), 847–849.



- 26 Y. Zhang, Y. H. Xu, M. H. Li, *et al.*, Growth and properties of Zn doped lithium niobate crystal, *J. Cryst. Growth*, 2001, **233**(3), 537–540.
- 27 F. Chen, Y. Tan and A. Ródenas, Ion implanted optical channel waveguides in Er<sup>3+</sup>/MgO co-doped near stoichiometric LiNbO<sub>3</sub>: a new candidate for active integrated photonic devices operating at 1.5 μm, *Opt. Express*, 2008, **16**(20), 16209–16214.
- 28 J. K. Yamamoto, Growth and characterization of Sc<sub>2</sub>O<sub>3</sub>-doped LiNbO<sub>3</sub>, *J. Cryst. Growth*, 1993, **128**(s 1–4), 920–923.
- 29 H. J. Chen, L. H. Shi, W. B. Yan, *et al.*, OH<sup>−</sup> absorption bands of LiNbO<sub>3</sub> with varying composition, *Chin. Phys. B*, 2009, **18**(6), 2372–2376.
- 30 Z. Zhou, B. Lin, S. Lin, *et al.*, Defect structure and nonvolatile hologram storage properties in Hf:Fe:Mn:LiNbO<sub>3</sub> crystals, *Optik*, 2011, **122**(13), 1179–1182.
- 31 P. Hou, Y. Zhi and J. Sun, Theoretical studies on dynamics of fixed holograms with high diffraction efficiency in Fe:LiNbO<sub>3</sub> crystals, *SPIE-Int. Soc. Opt. Eng.*, 2012, **8497**(12), 1109–1124.
- 32 L. Dai, Z. Yan, S. Jiao, *et al.*, OH<sup>−</sup> absorption and one-color holographic recording in Ru:Fe:LiNbO<sub>3</sub> crystals varied co-doped with HfO<sub>2</sub>, *Opt. Mater.*, 2014, **38**, 252–255.
- 33 Q. X. Xi, D. A. Liu, Y. N. Zheng, *et al.*, Electrochromic effect in domain-inversion process in LiNbO<sub>3</sub>: Ru: Fe crystals, *Chin. Sci. Bull.*, 2005, **50**(24), 2799–2803.

